Journal of Anatomy

J. Anat. (2010) **217**, pp16–25 doi: 10.1111/j.1469-7580.2010.01239.x

A comparative study of gland cells implicated in the nerve dependence of salamander limb regeneration

Anoop Kumar,[1] Graham Nevill,[2] Jeremy P. Brockes[1] and Andrew Forge[2]

[1]*Institute for Structural and Molecular Biology, University College London, London, UK*
[2]*Centre for Auditory Research, UCL Ear Institute, University College London, UK*

Abstract

Limb regeneration in salamanders proceeds by formation of the blastema, a mound of proliferating mesenchymal cells surrounded by a wound epithelium. Regeneration by the blastema depends on the presence of regenerating nerves and in earlier work it was shown that axons upregulate the expression of newt anterior gradient (nAG) protein first in Schwann cells of the nerve sheath and second in dermal glands underlying the wound epidermis. The expression of nAG protein after plasmid electroporation was shown to rescue a denervated newt blastema and allow regeneration to the digit stage. We have examined the dermal glands by scanning and transmission electron microscopy combined with immunogold labelling of the nAG protein. It is expressed in secretory granules of ductless glands, which apparently discharge by a holocrine mechanism. No external ducts were observed in the wound epithelium of the newt and axolotl. The larval skin of the axolotl has dermal glands but these are absent under the wound epithelium. The nerve sheath was stained post-amputation in innervated but not denervated blastemas with an antibody to axolotl anterior gradient protein. This antibody reacted with axolotl Leydig cells in the wound epithelium and normal epidermis. Staining was markedly decreased in the wound epithelium after denervation but not in the epidermis. Therefore, in both newt and axolotl the regenerating axons induce nAG protein in the nerve sheath and subsequently the protein is expressed by gland cells, under (newt) or within (axolotl) the wound epithelium, which discharge by a holocrine mechanism. These findings serve to unify the nerve dependence of limb regeneration.

Key words axolotl; blastema; Leydig cell; newt.

Introduction

Regeneration of the limb occurs in various species of salamanders including the adult newt (*Notophthalmus viridescens*) and the paedomorphic larval axolotl (*Ambystoma mexicanum*). Regeneration proceeds by formation of the limb blastema, a mound of mesenchymal stem cells that forms at the end of the stump (Brockes, 1997; Tsonis, 2000; Stocum, 2004). The division of the blastemal cells depends on the concomitant regeneration of axons in the major peripheral nerve branches of the limb (Tassava & Mescher, 1976; Brockes, 1984). Nerve dependence is a common feature of appendage regeneration in many contexts and may be a mechanism to ensure that the regenerate is functionally innervated (Brockes & Kumar, 2008). If the limb nerves are transected in the flank at the base of the limb, this prevents axonal regeneration and in turn prevents or arrests limb regeneration (Singer, 1952). The cellular and molecular mechanisms that link axonal regeneration to division of the blastemal cells have been unclear but recent work has implicated the newt anterior gradient (nAG) protein as playing a key role (Kumar et al. 2007). nAG protein expression in the limb is upregulated by regenerating axons as discussed below and it has the critical ability to rescue regeneration of a denervated blastema so that it can complete the proximodistal axis and form digits. The recombinant nAG protein acts as a mitogen for cultured limb blastemal cells by binding to its surface receptor, the glycosylphosphatidylinositol-anchored protein called Prod 1 (Morais da Silva et al. 2002; Kumar et al. 2007; Garza-Garcia et al. 2009). Anterior gradient proteins were discovered in studies on the development of the *Xenopus* tadpole cement gland (Sive et al. 1989) and the *Xenopus* protein XAG2 is able to induce an ectopic cement gland in addition to being expressed in the gland (Aberger et al. 1998). The proteins have a thioredoxin fold as well as an N-terminal signal sequence targeting them to the secretory pathway (Persson et al. 2005). They are widely expressed in vertebrates and are generally found

Correspondence
Dr Jeremy P. Brockes, ISMB, Darwin Building, UCL, Gower Street, London WC1E 6BT, UK. T: 0207 679 4483; E: j.brockes@ucl.ac.uk

Accepted for publication *22 March 2010*
Article published online *27 April 2010*

in secretory epithelia (Sive et al. 1989; Aberger et al. 1998; Kim et al. 2007; Kumar et al. 2007; Shih et al. 2007; Park et al. 2009; Xia et al. 2009). There is now an extensive literature on upregulation of anterior gradient proteins in mammalian adenocarcinoma (Thompson & Weigel, 1998; Fletcher et al. 2003; Barraclough et al. 2009) and the premalignant condition called Barrett's oesophagus (Pohler et al. 2004; Wang et al. 2008).

In a regenerating newt limb, the axonal processes extend along the nerve sheath. The Schwann cells of the distal sheath show strong expression of nAG protein at 5–7 days post-amputation and this is abrogated by prior denervation (Kumar et al. 2007). At 10–12 days the protein is expressed in glands in the dermis underlying the wound epithelium and also by some glands under the skin just proximal to the amputation plane. Interestingly, the generation of the glands is prevented by denervation. If nAG protein is expressed after electroporation in a denervated blastema, the secreted protein is able to induce the appearance of nAG protein-positive glands under the wound epithelium, an activity reminiscent of the *Xenopus* protein in relation to the cement gland (Aberger et al. 1998). It is likely that the appearance of the dermal glands during regeneration depends on the protein released by the Schwann cells contacted by regenerating axons and therefore is prevented by denervation. During the course of regeneration the wound epithelium differentiates into normal skin and the dermal glands lose expression of nAG protein (Kumar et al. 2007).

The activities of the nAG protein offer a new perspective on the role of gland cells in regeneration and raise a number of interesting issues. First, the most familiar configuration for amphibian glands is to discharge into a lumen ducted to the external surface of the skin where the secretions may play various roles (Fox, 1986). This would not be appropriate for a protein whose target is the mesenchymal blastema. Second, a number of salamander species are paedomorphic (neotenic) and among these the axolotl has been studied extensively as a model for regeneration (Kragl et al. 2009; Voss et al. 2009), including the aspect of nerve dependence (Tassava & Mescher, 1976; Endo et al. 2004; Satoh et al. 2009). The larval epidermis of the axolotl is different in several respects from the adult skin of the newt (Hay, 1961; Fahrmann, 1971b; Fox, 1986; Jarial, 1989). It features a glandular element, the Leydig cell, which is lost after thyroxine-induced metamorphosis (Fahrmann, 1971a). Furthermore, the wound epithelium of the axolotl limb blastema appears not to have the underlying dermal glands described in the newt, even though such glands are present under the normal epidermis (Le Quang Trong, 1967; Holder & Glade, 1984). We have explored these issues in more detail using antibodies against both nAG and axolotl anterior gradient (aAG) proteins, and employing transmission and scanning electron microscopy in addition to light microscopy.

Materials and methods

Animals and husbandry

Adult newts *(N. viridescens)* were obtained from Charles D. Sullivan & Co. (TN, USA) and maintained in the animal facility. For regeneration experiments, bilateral amputation of the forelimb was performed at mid-humerus level as described previously (Kumar et al. 2007) and the newts were maintained at 24 °C in a temperature-controlled facility. Axolotls were purchased from Neil Hardy Aquatica (Croydon, UK) and maintained at 18 °C throughout the experiments. Axolotls of various sizes [small (5 cm, snout to tail tip), medium (8–10 cm) and large (14–16 cm] were used in various experiments. Bilateral amputation of the forelimb was performed as for newts and the animals were maintained in individual containers. For axolotls, denervation of the limb was performed under anaesthesia as described previously (Tassava & Mescher, 1976). Briefly, the brachial plexus of the right forelimb was exposed and transection of the nerve branches was performed above the brachial plexus. In small and mid-sized animals the wound surface was sealed with a wounding adhesive, whereas in large axolotls the wound was closed using ophthalmic micro sutures. The animals were returned to individual containers for recovery. Amputation of the right denervated and left control limbs was carried out at 72 h after denervation and the animals were allowed to regenerate.

Tissue processing and histology

The limb blastema was collected from animals and fixed in 2.5% glutaraldehyde in 0.1 M cacodylate buffer (pH 7.3) for 2 h at room temperature (25°C). The fixed tissues were washed twice in 0.1 M cacodylate buffer, dehydrated and embedded in Histocryl (Leica, Wetzlar, Germany) following the manufacturer's instructions. The sections were cut on a rotary automatic microtome (RM 2155; Leica) at 2–4 μm thickness, collected on Superfrost plus slides, dried and stained with toludine blue.

Scanning electron microscopy

The limb blastema with the stump was collected and fixed by immersion in 2.5% glutaraldehyde in 0.1 M cacodylate buffer with 3 mM $CaCl_2$ for 2 h. After rinsing in the buffer, the samples were post-fixed in 1% OsO_4 in cacodylate buffer for 2 h at room temperature. Samples were then processed twice with thiocarbohydrazide followed by OsO_4 (Davies & Forge, 1987), before dehydration in an ethanol series and critical point drying. Samples were mounted on scanning electron microscope stubs using silver paint as adherent and then sputter-coated with platinum. The samples were examined in a JEOL 6700 field emission scanning electron microscope (JEOL (UK) Ltd, Welwyn Garden City, UK) operating at 3 or 5 kV.

Transmission electron microscopy

The limb blastema was collected without the stump tissue and fixed as described above. During dehydration in an ethanol series, the tissues were en-bloc stained in saturated uranyl acetate in 70% ethanol overnight, before continuing with dehydration followed by embedding. Thin sections were cut and stained

with uranyl acetate and lead citrate. At least one set of sections from each sample was mounted on formvar-coated single-slot grids to allow uninterrupted examination of the entire epithelium of the sample.

Immunogold labelling

The limb blastema samples were fixed by immersion in freshly prepared 4% paraformaldehyde containing 0.025% glutaraldehyde for 2 h at room temperature. The tissues were dehydrated to 100% ethanol and during dehydration the samples were cooled in stages to −30 °C in a freeze-substitution device. The samples were embedded in Lowicryl K4M and polymerized under UV light at −30 °C. Thin sections were mounted on nickel grids and the grids were floated on a droplet of 10% goat serum containing 0.15% Tween-20 in phosphate-buffered saline (PBS) for 1–2 h. The grids were reacted with the primary antibody (nAG peptide antibody 223), diluted 1 : 50 in 100 mM lysine in PBS with 0.15% Tween, overnight at 4 °C. After washes in PBS-Tween, the sections were incubated in goat anti-rabbit secondary antibody conjugated to 10-nm gold particles at a dilution of 1 : 50. They were then exposed briefly to 0.1% glutaraldehyde in PBS followed by washing in distilled water. Sections were counterstained with uranyl acetate and lead citrate. For negative controls, the primary antibody was omitted or the sections were reacted with concentration-matched non-specific primary rabbit antibody.

Antibodies and immunofluorescence staining

Peptide antibody to aAG protein was raised in rabbit. Rabbits were immunized (Eurogentec, Seraing, Belgium) with Keyhole Limpet Hemocyanin conjugated to peptides for amino acids 20–34 (reagent 398) and 132–147 (reagent 399) of the aAG protein sequence and the sera were affinity purified by adsorption and elution from the appropriate immobilized peptide (Eurogentec). The specificity of the antibody was assayed in cross-sections of the axolotl limb tissue (see Results).

The tissues were fixed in 4% paraformaldehyde overnight at 4 °C. The samples were washed in PBS and embedded in Tissue-Tek (Sakura Finetek, Thatcham, UK). Serial longitudinal or cross-sections were cut in a cryostat at 12 μm, collected on Superfrost plus slides (Thermo-Fisher Scientific, Loughborough, UK) and air dried at room temperature for 15 min. The slides were rinsed in PBS to remove the embedding media and incubated in PBS containing 0.2% Triton-x100 for 10 min. Tissue samples were

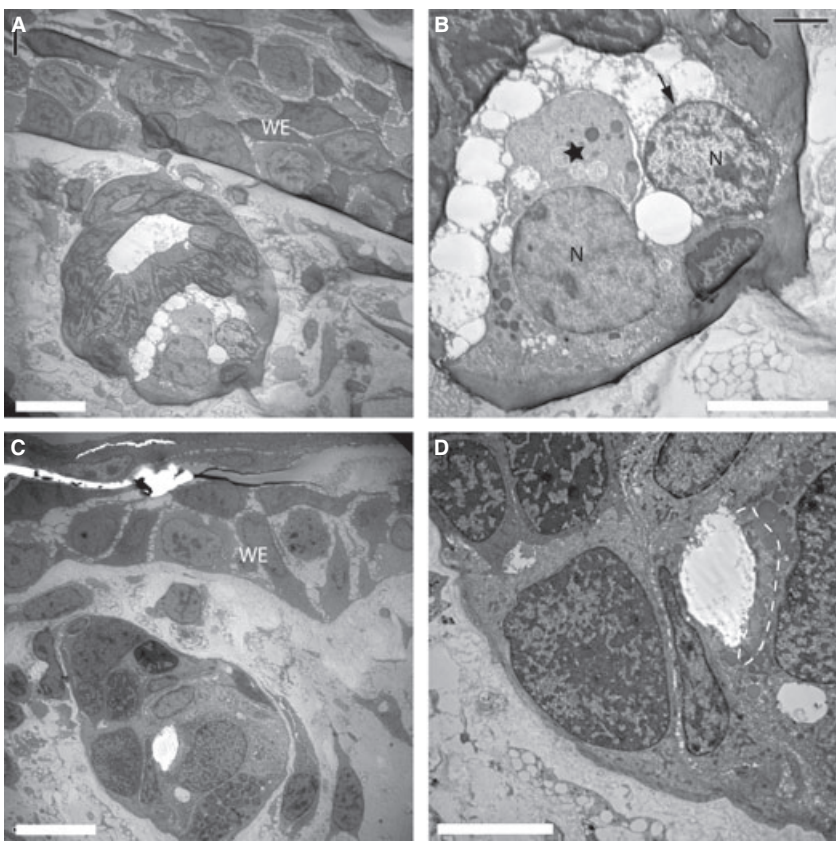

Fig. 1 Ultrastructure of glands under the wound epithelium (WE) of the newt limb blastema. (A) A gland that has formed under the WE at 12 days post-amputation. (B) A higher magnification image of the gland in (A). A single cell (asterisk) is discharging its contents into the extracellular space, whereas another cell (arrowed) has discharged its contents. (C) A more mature gland under the proximal WE. The morphology resembles the adult gland type and is associated with the progressive differentiation of the regenerate. (D) A higher magnification of the gland in (C) showing secretory granules with moderate electron density (dotted line) that have accumulated at the leading edge of the cell. N, nucleus. Scale bars: 20 μm (A and C) and 10 μm (B and D).

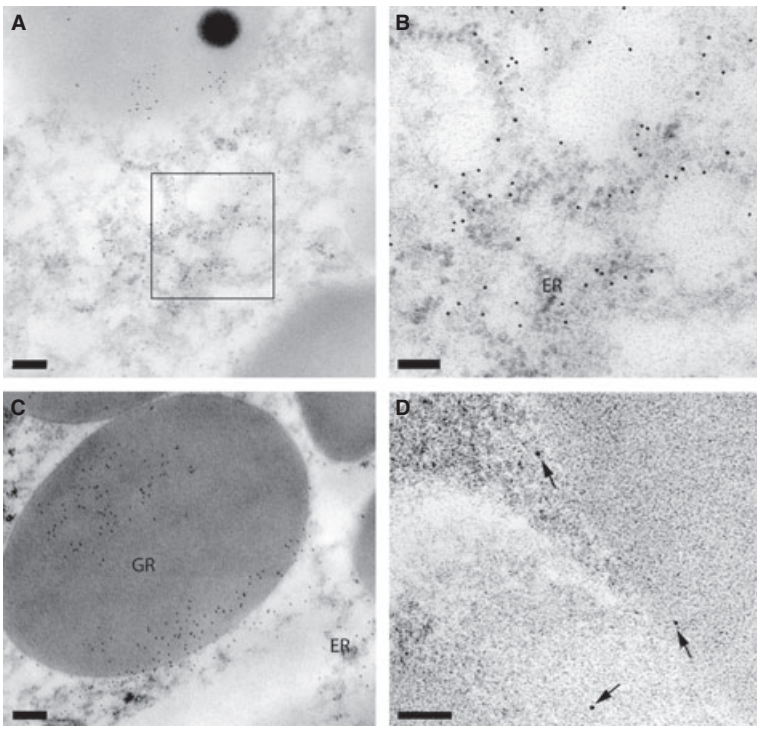

Fig. 2 Immunogold labelling of the newt anterior gradient (nAG) protein in dermal glands of a newt limb blastema. (A) Section of a gland after reaction with rabbit antibodies to nAG protein, followed by gold-labelled anti-immunoglobulin reagent. Gold particles are visible in the secretory granules and cytoplasm. (B) A higher magnification of the boxed area from (A) showing labelling of the endoplasmic reticulum (ER). (C) A high-magnification image of a granule (GR) showing gold labelling. (D) A section after reaction with a non-specific antibody shows little or no reaction with the gland cells. An occasional gold particle is visible (arrowed). Scale bars: 0.2 μm (A and D) and 0.5 μm (B and C).

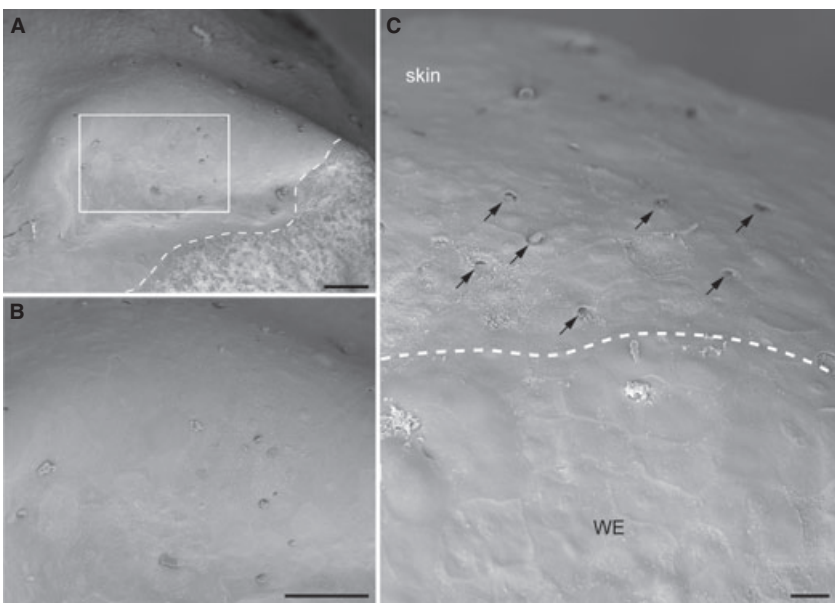

Fig. 3 Scanning electron micrograph of wound epithelium (WE) in the newt blastema. (A) Low-power scanning electron microscopy of a newt limb blastema at 12 days post-amputation. The dotted line indicates the boundary of the sample and conductive silver paint. (B) A higher magnification view of the boxed area from (A) showing the surface of the WE of the limb blastema. Unlike adult skin, the WE is devoid of any glandular openings. (C) An area showing the boundary between the limb stump and regeneration blastema. The dotted line demarcates the old skin from the WE. Note the presence of glandular openings in the old skin (arrows), which is entirely absent in the WE. Scale bars: 100 μm (A and B) and 20 μm (C).

blocked in PBS containing 10% goat serum for 45 min. Primary antibody (aAG peptide antibody 398) was diluted in PBS containing 10% goat serum at 1 : 200 and spun in a centrifuge at 20 500 *g* for 15 min. The slides with primary antibody were incubated overnight at 4 °C in a humidified chamber. The slides were washed twice in PBS and reacted with Alexa 488 goat anti-rabbit secondary antibody (Invitrogen, Paisley, UK) at 1 : 500 dilution for 1 h. Sections were further washed in PBS and the nuclei were counterstained with Hoechst 33258 (2 μg mL^{-1}). The slides were mounted in Dako (Ely, UK) fluorescent mounting medium.

For localization of serotonin in axolotl limbs, the tissues were processed as above and reacted with anti-serotonin, clone YC5/45 rat monoclonal antibody (Millipore, Watford, UK) at 1 : 75 dilution for 4 h at room temperature. Alexa 488 goat anti-rat antibody (Invitrogen) was used as the secondary layer at 1 : 250 dilution. In double-immunofluorescence staining to localize aAG protein- and serotonin-reactive cells, Alexa 568 goat anti-rabbit antibody was employed to identify the aAG protein reactivity in tissues. The slides were observed under a Zeiss (Welwyn Garden City, UK) Axioskop 2 microscope and the images were acquired using an Orca ER digital camera (Hamamatsu Photonics, Welwyn Garden City, UK) driven by Openlab software (Perkin Elmer, Cambridge, UK). For analysis of control and denervated limb tissues, the images were acquired with identical camera settings and illumination. Post-processing of the images was performed in Openlab and the images were exported to Adobe Photoshop 7.0 for further processing.

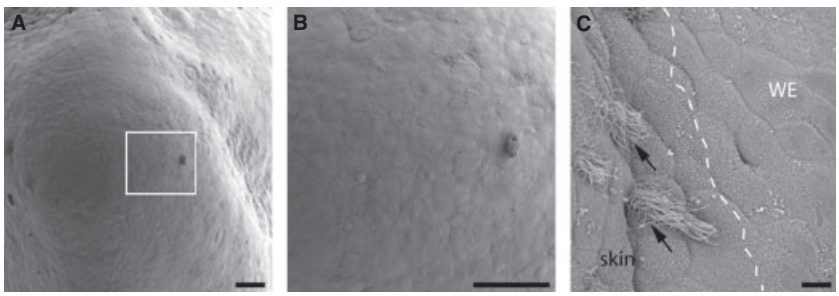

Fig. 4 Scanning electron micrograph showing the surface features of an axolotl limb blastema. (A) Low-magnification view of an axolotl limb blastema. (B) Boxed area from (A), showing the surface morphology of the wound epithelium (WE). Note the nature of the smooth WE lacking any glandular openings. (C) A magnified area showing the boundary between the limb stump and regeneration blastema. The skin of the limb stump has ciliated glandular pores (arrows), whereas the WE lacks any glands. Scale bars: 100 μm (A and B) and 10 μm (C).

A

```
                                        398
axoAGR MATCHLSALVLLVLSSHGMAKDNGKKPEVKKVQTLSRGWGDSLEWVQTYE 50
   nAG MVKGYLAALLLLALSSFSLAKESAKRPEVKKVQTLSRGWGDSLEWAQTYE

axoAGR EGLFKAKNSNKPLMVINHRDDCPHSQALKKTFAEHKGIQKIAEKFILLNI 100
   nAG ESLSKSRSSNKPLLVINHRDDCPHSQALKKAFAEHKGIQKLAEKFILLNV
                                                399
axoAGR VHDPTDKNLLLDGLYVPKIIFVDPSMVVRADIPGKYSNHRYTYEPTDCDL 150
   nAG VHDPTDKNLVLDGMYVPKLVFVDPSMVVRADLPGKYSNHRYTYEPADIDL

axoAGR LFENMKKALKLLKTEL 166
   nAG LYGNMQKALKLLKTEL
```

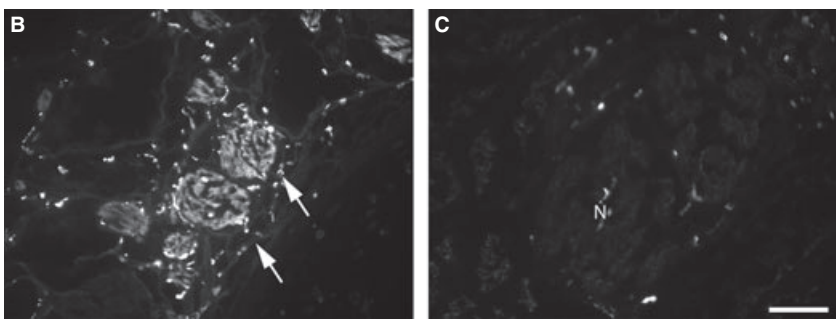

Fig. 5 Axolotl anterior gradient (aAG) protein. (A) Alignment showing the amino acid sequence of the aAG protein with newt anterior gradient protein. Highlighted amino acids represent the two peptides, 398 and 399, which were used as immunogens to raise antibodies in rabbits. (B) A section of nerve bundles in an axolotl forelimb (arrows) after reaction with the 398 antibody and detection by indirect immunofluorescence. Note the specific reactivity of the antibody to nerve bundles. (C) Immunoreactivity of a non-specific rabbit antibody reacted at a matched concentration to (B) in a cross-section of axolotl forelimb. N, nerve. Scale bars: 200 μm (B and C).

Results

The dermal glands under the wound epithelium of the regenerating newt limb were analysed by electron microscopy. A representative example of such a gland at 12 days post-amputation is shown in Fig. 1A. The gland is suspended in the dermis and no ducts were observed that connect it to the overlying wound epithelium. This has been confirmed by analysing serial sections of such glands. The images of granular discharge and loss of cell contents are consistent with a mode of holocrine release shown at higher power in Fig. 1B. As the regenerate undergoes progressive differentiation the glands under the epithelium take on a more adult morphology (Fig. 1C,D). The dermal glands under the skin of a normal newt limb were analysed both by light (Fig. S1) and electron (Fig. S2) microscopy, and were consistent with images of mucous and serous (granular) glands previously described in adult salamander species (Le Quang Trong, 1967; Holder & Glade, 1984; Fox, 1986; Reyer et al. 1992). It was not possible to unambiguously relate the gland shown in Fig. 1A to a type in normal skin but the absence of ducts suggests that it may not be a mucous gland.

The dermal glands under the wound epithelium were further analysed by reacting sections with rabbit antibodies to a peptide sequence in newt nAG protein, followed by gold-labelled anti-rabbit antibodies. Gold particles were observed over both the granules and the endoplasmic reticulum, consistent with the secreted identity of the nAG protein (Fig. 2A–C). When sections were reacted with control rabbit antibodies at the same concentration, followed by the gold-labelled reagent, there were comparatively few gold particles (Fig. 2D). The specific immunogold labelling confirms that the ultrastructural images correspond to the nAG protein-positive glands previously observed by immunofluorescence (Kumar et al. 2007).

The external surface of the limb blastema was imaged by scanning electron microscopy and views of the 12-day blastema are shown in Fig. 3A–C. The wound epithelium was devoid of any glandular openings, in contrast to the normal skin which showed, as expected, an array of such openings (Fig. 3C). This is consistent with the absence of ducted glands in the dermal layer of the wound epithelium. The axolotl limb blastema was analysed by scanning microscopy and it also showed an absence of openings in the wound epithelium, whereas the larval skin showed ciliated glandular pores (Fig. 4A–C).

The amino acid sequence for the nAG protein orthologue in the axolotl (aAG protein) is shown in Fig. 5A and is 83% identical to nAG protein. Two antibodies, denoted 398 and 399, were raised against peptides from the aAG protein sequence and tested on sections of axolotl limb. Reagent 398 showed specific staining of peripheral nerve bundles as compared with control rabbit antibodies (Fig. 5B,C) and

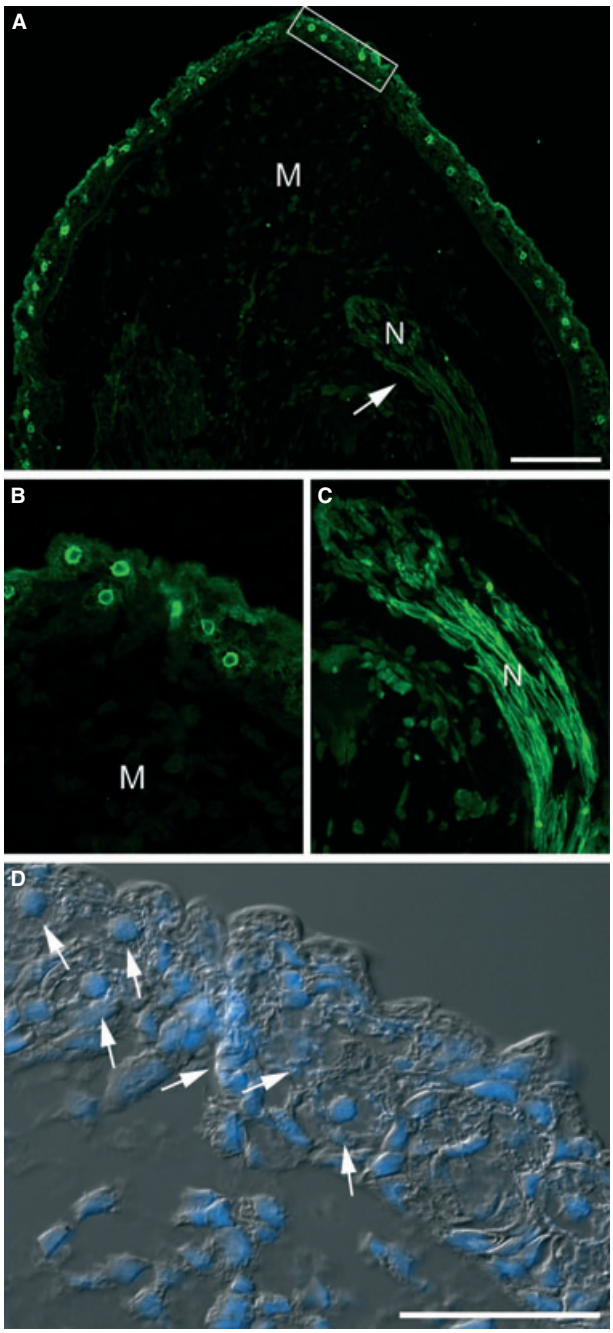

Fig. 6 Localization of axolotl anterior gradient (aAG) protein in the axolotl limb blastema by indirect immunofluorescence. (A) Expression of aAG protein in a section of a blastema at 11 days post-amputation. Note the reactivity of the nerve sheath as well as cells in the wound epithelium and the general lack of reactivity in mesenchymal cells. (B) A higher magification image of the boxed area from (A). Note the characteristic reactivity with a subset of cells. (C) Higher magnification image of the nerve sheath from (A). (D) A composite overlay of the boxed area in (A) using differential interference contrast and the nuclear stain Hoechst 33258. The arrows identify the cells expressing aAG protein in (B). M, mesenchyme; N, nerve. Scale bars: 200 μm (A) and 50 μm (D).

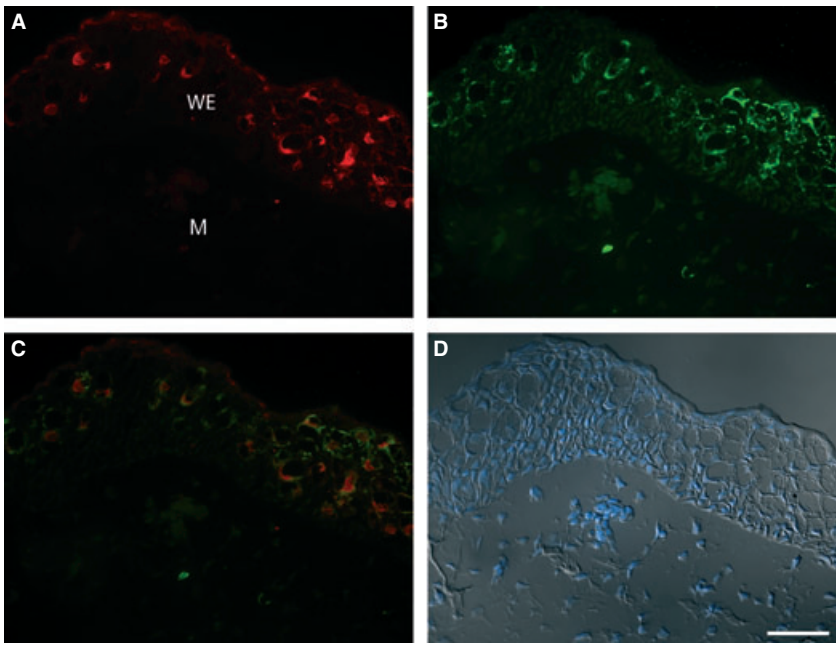

Fig. 7 Localization of axolotl anterior gradient (aAG) protein and serotonin in Leydig cells of the wound epithelium by double fluorophor immunofluorescence. (A) Expression of aAG protein detected with rabbit antibody 398. (B) Expression of serotonin in Leydig cells detected with rat monoclonal anti-serotonin. (C) Composite overlay showing that serotonin-positive Leydig cells express aAG protein. (D) Composite overlay of differential interference contrast and nuclear dye showing morphological features of the wound epithelium. WE, wound epithelium; M, mesenchyme. Scale bars: 200 μm (A–D).

was selected for further study. In sections of the 11-day axolotl limb blastema, the antibody reacted with the nerve sheath cells (Fig. 6A,C) and with distinctive cells in the wound epithelium with the appearance of Leydig cells (Fig. 6A,B). The wound epithelium was analysed by electron microscopy (Fig. S3A) and characteristic images of Leydig cells in early (Fig. S3B) and late (Fig. S3C) stages of holocrine secretion were observed as described previously (Jarial, 1989).

Leydig cells have been reported to stain with antibodies to serotonin (Toyoshima & Shimamura, 1992) and when the wound epithelium was double stained with antibodies to aAG protein and serotonin there was a close correspondence of staining in these cells, although the antigens appeared to be in distinct locations within the cell (Fig. 7A–D). The co-expression of aAG protein and serotonin in Leydig cells of the normal epidermis was also observed (Fig. S4). No staining for serotonin was observed in the adult newt skin or wound epithelium.

Dermal glands were observed in the skin of the normal axolotl limb (Fig. S5A) but not under the wound epithelium, in contrast to the newt (Fig. S5C). Glands were found in the dermis just proximal to the amputation plane (Fig. S5B). Such glands were stained by the 398 antibody, as shown for the 9-day regenerate (Fig. S6A,B), but were unlabelled in the contralateral limb that was denervated prior to amputation (Fig. S6C,D). The nerve sheath cells showed strong reactivity with the antibody in the innervated blastema, whereas the sheath in the contralateral denervated blastema was negative as noted previously in the newt (Kumar et al. 2007).

The effect of denervation on aAG protein expression by Leydig cells in the wound epithelium was analysed in an experiment where axolotl limbs were denervated unilaterally at 72 h prior to bilateral amputation. The innervated limb showed strong antibody reactivity at 9 days post-amputation as before but this was greatly diminished in sections from the contralateral denervated limb processed in parallel (Fig. 8A,B). This decrease did not result from the absence of Leydig cells in the denervated wound epithelium as these cells could be readily observed by staining with antibody to serotonin (data not shown). These experiments were performed on mid-sized (8–10 cm) larvae. We noted that the wound epidermis of larger (14–16 cm) larvae showed low antibody labelling of both innervated and denervated blastemas.

Discussion

The ultrastructural analysis of the regenerating adult newt limb has extended the earlier findings on the dermal glands that express nAG protein. The protein is expressed in the secretory granules of cells that apparently discharge their contents in close proximity to the mesenchymal blastema. The images from both transmission and scanning electron microscopy indicate that the glands underlying the wound epithelium are not ducted to the exterior surface. It is not clear if the nAG protein-positive glands correspond to a

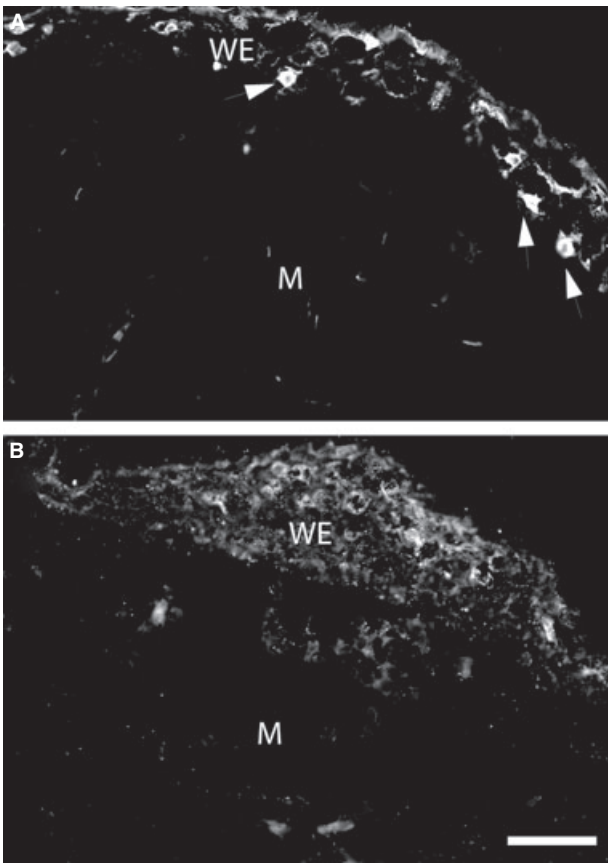

Fig. 8 Effect of denervation on expression of axolotl anterior gradient (aAG) protein in the axolotl wound epithelium. (A) Section of the wound epithelium from an axolotl blastema at 9 days post-amputation showing aAG protein-positive cells (arrowheads) detected by indirect immunofluorescence. (B) Section of the blastema from the contralateral limb denervated 72 h prior to amputation. Note the absence of positive cells in the wound epithelium. WE, wound epithelium; M, mesenchyme. Scale bars: 200 μm (A and B).

particular population in the normal skin, as the appearance of the serous glands is quite variable at different stages of maturation and secretion. The earlier study presented evidence that the dermal glands of the wound epidermis arise as a result of the activity of the nAG protein released by Schwann cells associated with regenerating axons (Kumar et al. 2007). The presence of this protein in the nerve sheath has also been observed in relation to axolotl limb regeneration in the present study and this critical aspect of nerve dependence is therefore conserved. The dermal glands are present in the normal epidermis of the axolotl and glands located at the proximal boundary of the wound epithelium upregulate the expression of nAG protein in an innervated limb. Nonetheless, the absence of these glands under the wound epidermis is a distinction between newt and axolotl as described in the Introduction.

Leydig cells are associated with the epidermis of larval salamanders and are lost after metamorphosis (Hay, 1961; Kelly, 1966; Fahrmann, 1971a,b; Jarial, 1989). They continue to be present in paedomorphic species such as the axolotl, as well as after experimental arrest of metamorphosis (Ohmura & Wakahara, 1998). Although the morphological features of these cells have been described in detail, the functional role of their secretory products is unclear (Hay, 1961; Warburg & Lewinson, 1977; Fox, 1986; Jarial, 1989; Reyer et al. 1992). It is therefore a significant finding that the Leydig cells of the normal epidermis and wound epithelium express the orthologous anterior gradient protein. The holocrine release of their contents, which was observed earlier (Jarial, 1989) and is confirmed here, is appropriate for activity on the cells of the mesenchymal blastema. The effect of limb denervation on the wound epithelium is to downregulate the expression of aAG protein in the Leydig cells but not to induce the loss or non-appearance of these cells. Interestingly, the denervation of a normal (non-amputated) limb led to no change in aAG protein expression in the epidermis. In an earlier study, denervation of the sacral plexus in *Ambystoma tigrinum* induced progressive degeneration of Leydig cells (Hui & Smith, 1976) but this was not observed with brachial denervation in the axolotl. It is important to note that the Leydig cells in the wound epithelium could be derived by differentiation of progenitors in this location or alternatively by migration of mature cells from the wound edges of the epidermis. It is more straightforward to interpret the nerve dependence in terms of an effect of nAG protein on differentiation but this is a question that will require further investigation. Nonetheless, the present findings serve to bring the overall mechanism of nerve dependence of limb regeneration into register between the newt and axolotl. In both species the regenerating axons induce anterior gradient protein expression in the nerve sheath and thereafter the protein appears in gland cells associated with the wound epithelium that release by a holocrine mechanism. The protein acts directly on the mesenchymal cells of the blastema to stimulate division, as shown by its action on primary cells in culture (Kumar et al. 2007). The present findings should provide a framework for further studies on the establishment of nerve dependence during embryonic and larval development.

Acknowledgements

This work was supported by an MRC Programme Grant and MRC Research Professorship to J.P.B. We thank P. Gates for his help with the cloning of aAG protein.

References

Aberger F, Weidinger G, Grunz H, et al. (1998) Anterior specification of embryonic ectoderm: the role of the Xenopus cement gland-specific gene XAG-2. *Mech Dev* **72**, 115–130.

Barraclough DL, Platt-Higgins A, de Silva Rudland S, et al. (2009) The metastasis-associated anterior gradient 2 protein is correlated with poor survival of breast cancer patients. *Am J Pathol* **175**, 1848–1857.

Brockes JP (1984) Mitogenic growth factors and nerve dependence of limb regeneration. *Science* **225**, 1280–1287.

Brockes JP (1997) Amphibian limb regeneration: rebuilding a complex structure. *Science* **276**, 81–87.

Brockes JP, Kumar A (2008) Comparative aspects of animal regeneration. *Annu Rev Cell Dev Biol* **24**, 525–549.

Davies S, Forge A (1987) Preparation of the mammalian organ of Corti for scanning electron microscopy. *J Microsc* **147**, 89–101.

Endo T, Bryant SV, Gardiner DM (2004) A stepwise model system for limb regeneration. *Dev Biol* **270**, 135–145.

Fahrmann W (1971a) Morphodynamics of the axolotl epidermis (Siredon mixicanum Shaw) under the influence of exogenously applied thyroxin. 3. Epidermis of the metamorphosed axolotl. *Z Mikrosk Anat Forsch* **84**, 1–25.

Fahrmann W (1971b) Morphodynamics of the epidermis of the axolotl (Sideron mexicanum Shaw) under the influence of exogenous by administered thyroxine. I. Epidermis of neotenic axolotl. *Z Mikrosk Anat Forsch* **83**, 472–506.

Fletcher GC, Patel S, Tyson K, et al. (2003) hAG-2 and hAG-3, human homologues of genes involved in differentiation, are associated with oestrogen receptor-positive breast tumours and interact with metastasis gene C4.4a and dystroglycan. *Br J Cancer* **88**, 579–585.

Fox H (1986) The skin of amphibia. In *Biology of the Integument. 2 Vertebrates* (eds Bereiter-Hahn J, Matoltsy AG, Richards KS), pp. 78–148. Berlin, Heidelberg: Springer-Verlag.

Garza-Garcia A, Harris R, Esposito D, et al. (2009) Solution structure and phylogenetics of Prod1, a member of the three-finger protein superfamily implicated in salamander limb regeneration. *PLoS ONE* **4**, e7123.

Hay ED (1961) Fine structure of an unusual intracellular supporting network in the Leydig cells of Amblystoma epidermis. *J Biophys Biochem Cytol* **10**, 457–463.

Holder N, Glade R (1984) Skin glands in the axolotl: the creation and maintenance of a spacing pattern. *J Embryol Exp Morphol* **79**, 97–112.

Hui FW, Smith AA (1976) Degeneration of Leydig cells in the skin of the salamander treated with cholinolytic drugs or surgical denervation. *Exp Neurol* **53**, 610–619.

Jarial MS (1989) Fine structure of the epidermal Leydig cells in the axolotl Ambystoma mexicanum in relation to their function. *J Anat* **167**, 95–102.

Kelly DE (1966) The Leydig cell in larval amphibian epidermis. Fine structure and function. *Anat Rec* **154**, 685–699.

Kim NS, Shen YN, Kim TY, et al. (2007) Expression of AGR-2 in chicken oviduct during laying period. *J Biochem Mol Biol* **40**, 212–217.

Kragl M, Knapp D, Nacu E, et al. (2009) Cells keep a memory of their tissue origin during axolotl limb regeneration. *Nature* **460**, 60–65.

Kumar A, Godwin JW, Gates PB, et al. (2007) Molecular basis for the nerve dependence of limb regeneration in an adult vertebrate. *Science* **318**, 772–777.

Le Quang Trong NY (1967) Histogenèse et histochimie des glandes cutanées de l'axolotl (*Ambystoma tigrinum* Green). *Arch Zool Exp Gen (Paris)* **108**, 49–75.

Morais da Silva S, Gates PB, Brockes JP (2002) The newt ortholog of CD59 is implicated in proximodistal identity during amphibian limb regeneration. *Dev Cell* **3**, 547–555.

Ohmura H, Wakahara M (1998) Transformation of skin from larval to adult types in normally metamorphosing and metamorphosis-arrested salamander, Hynobius retardatus. *Differentiation* **63**, 238–246.

Park SW, Zhen G, Verhaeghe C, et al. (2009) The protein disulfide isomerase AGR2 is essential for production of intestinal mucus. *Proc Natl Acad Sci USA* **106**, 6950–6955.

Persson S, Rosenquist M, Knoblach B, et al. (2005) Diversity of the protein disulfide isomerase family: identification of breast tumor induced Hag2 and Hag3 as novel members of the protein family. *Mol Phylogenet Evol* **36**, 734–740.

Pohler E, Craig AL, Cotton J, et al. (2004) The Barrett's antigen anterior gradient-2 silences the p53 transcriptional response to DNA damage. *Mol Cell Proteomics* **3**, 534–547.

Reyer RW, Liou W, Pinkstaff CA (1992) Morphology and glycoconjugate histochemistry of the palpebral glands of the adult newt, Notophthalmus viridescens. *J Morphol* **211**, 165–178.

Satoh A, James MA, Gardiner DM (2009) The role of nerve signaling in limb genesis and agenesis during axolotl limb regeneration. *J Bone Joint Surg Am* **91**(Suppl 4), 90–98.

Shih LJ, Lu YF, Chen YH, et al. (2007) Characterization of the agr2 gene, a homologue of X. laevis anterior gradient 2, from the zebrafish, Danio rerio. *Gene Expr Patterns* **7**, 452–460.

Singer M (1952) The influence of the nerve in regeneration of the amphibian extremity. *Q Rev Biol* **27**, 169–200.

Sive HL, Hattori K, Weintraub H (1989) Progressive determination during formation of the anteroposterior axis in Xenopus laevis. *Cell* **58**, 171–180.

Stocum DL (2004) Amphibian regeneration and stem cells. *Curr Top Microbiol Immunol* **280**, 1–70.

Tassava RA, Mescher AL (1976) Mitotic activity and nucleic acid precursor incorporation in denervated and innervated limb stumps of axolotl larvae. *J Exp Zool* **195**, 253–262.

Thompson DA, Weigel RJ (1998) hAG-2, the human homologue of the Xenopus laevis cement gland gene XAG-2, is coexpressed with estrogen receptor in breast cancer cell lines. *Biochem Biophys Res Commun* **251**, 111–116.

Toyoshima K, Shimamura A (1992) Leydig cells in the lingual epithelium of the axolotl, Ambystoma mexicanum, are immunoreactive for serotonin. *J Anat* **181**, 365–367.

Tsonis PA (2000) Regeneration in vertebrates. *Dev Biol* **221**, 273–284.

Voss SR, Epperlein HH, Tanaka EM (2009) *Ambystoma mexicanum*, the axolotl: a versatile amphibian model for regeneration, development, and evolution studies. *Cold Spring Harb Protoc* 2009, doi:10.1101/pdb.emo128.

Wang Z, Hao Y, Lowe AW (2008) The adenocarcinoma-associated antigen, AGR2, promotes tumor growth, cell migration, and cellular transformation. *Cancer Res* **68**, 492–497.

Warburg MR, Lewinson D (1977) Ultrastructure of epidermis of Salamandra salamandra followed throughout ontogenesis. *Cell Tissue Res* **181**, 369–393.

Xia J-H, Jiang J, Shi Y-H, et al. (2009) Predominant expression and cellular distribution of fish Agr2 in renal collecting system. *Comp Biochem Physiol B Biochem Mol Biol* **152**, 397–404.

Supporting information

Additional Supporting Information may be found in the online version of this article:

Fig. S1 Light microscopic morphology of the dermal glands in the skin of adult newts. (A) An area of the skin showing different dermal glands. The glands with dense vesicles (white arrow) are similar, except that one of them shows a regressive morphology corresponding to the secretory cycle of the gland. The second type of gland (black arrow) does not show any clear vesicles or granules. (B) Of the three glands present here, two (white arrow) show morphology similar to that of glands in (A), whereas the third type of gland (black arrow) appears distinct. E, epidermis; D, dermis. Scale bars: 100 μm (A and B).

Fig. S2 Transmission electron micrograph of dermal glands in the adult newt skin. (A) Low-magnification montage of a dermal gland showing accumulation of granules of light and dense electron density towards the lower section of the gland. The upper part of the gland shows large vesicles. The association of vesicles to individual cells is not clear in the gland. (B) Example of another gland with a different vesicular morphology. A lumen is present in this gland and the nucleus of each cell is arranged towards the periphery of the gland. (C) Another gland from the newt dermis showing a large accumulation of glandular vesicles. The secretory material in these vesicles is of more amorphous nature compared with the other types of glands. (D), (E) and (F) Higher magnification of the boxed areas from (A), (B) and (C), respectively. Scale bars: 10 μm (A–C and F) and 5 μm (D and E).

Fig. S3 Morphological features of the wound epithelium of an axolotl limb blastema. (A) Low-magnification transmission electron microscopy (TEM) of the distal tip of a wound epithelium. The arrows indicate Leydig cells at two phases of secretion. (B) A cell in (A) (lower white arrow) is magnified to show its morphology. The cell is at an early stage of the secretory cycle showing a clear nucleus and accumulation of granules of varying density, as well as vacuoles. (C) A Leydig cell at a late stage of secretion. The cell has emptied most of its contents by its holocrine secretory mechanism. Scale bars: 50 μm (A) and 5 μm (B and C).

Fig. S4 Expression of axolotl anterior gradient (aAG) protein and serotonin in the skin of an axolotl limb. (A) Expression of aAG protein in epidermal Leydig cells proximal to the amputation plane of a limb blastema. (B) The section of (A) showing reactivity of Leydig cells to antibody to serotonin. (C) Composite overlay of (A) and (B) showing that Leydig cells express aAG protein. (D) Composite overlay of differential interference contrast and the nuclear stain showing morphology of cells. E, epidermis. Scale bar: 200 μm (A–D).

Fig. S5 Dermal glands in normal and regenerating limbs of axolotls. (A) Light microscopic image of dermal glands in the dermis of axolotl (arrows). (B) A developing gland in the proximal region of the limb blastema in axolotl (arrow). These glands develop from the basal layer of the differentiating wound epithelium and submerge into the mesenchyme during limb blastema differentiation. (C) Low-magnification image of a limb blastema of axolotl. Note the absence of any glandular structures under the wound epithelium. E, epidermis; D, dermis; M, mesenchyme; WE, wound epithelium. Scale bars: 100 μm (A and B) and 200 μm (C).

Fig. S6 Immunofluorescence staining of dermal glands in axolotl. (A) A dermal gland showing reactivity to axolotl anterior gradient (aAG) protein in a 9-day-old limb blastema. The gland is located proximal to the amputation plane of the limb. (B) A composite overlay of differential interference contrast and nuclear stain, showing the morphological features of the gland in (A). (C) Section of the denervated contralateral limb. The glands proximal to the amputation plane of the limb are nonreactive to the antibody against aAG protein. (D) A composite overlay of the glands shown in (C). E, epidermis; D, dermis. Scale bar: 200 μm (A–D).

As a service to our authors and readers, this journal provides supporting information supplied by the authors. Such materials are peer-reviewed and may be re-organized for online delivery, but are not copy-edited or typeset. Technical support issues arising from supporting information (other than missing files) should be addressed to the authors.